Oligoaniline Complexes

Self-Assembly and Electrical Conductivity Transitions in Conjugated Oligoaniline–Surfactant Complexes**

*Zhixiang Wei, Teija Laitinen, Bernd Smarsly, Olli Ikkala, and Charl F. J. Faul**

Building well-ordered two- and three-dimensional nanostructures in a facile way is essential for the next generation of electrical, optical, and magnetic materials and devices.[1] Molecular self-assembly[2] is a versatile method to prepare such structures by binding mutually repulsive groups with attractive interactions, for example, ionic interactions, hydrogen bonding, van der Waals forces, and metal coordination.[3] Besides precise control over the structures, self-assembly can also lead to properties that can be controlled by external conditions.[4] Conjugated oligomers have been used for electroactive materials and devices,[5] and here we show that conjugated aniline tetramers and octamers are able to form well-defined 2D self-assembled columnar structures upon ionic complexation with di(*n*-alkyl) phosphate surfactants. This behavior is in contrast to the corresponding polyaniline (PANI) complexes that form 2D hexagonally arranged assemblies. Importantly, order–disorder transitions are observed as reversible transitions in electrical conductivity as a function of temperature. Therefore, this self-assembly strategy allows for responsive electroactive properties of conjugated materials.

PANI salts, which are both electrically conducting conjugated polymers and polyelectrolyte complexes, can form lamellar or hexagonal nanostructures through ionic self-assembly with surfactants or hydrogen-bonded amphiphiles.[6] However, as with most self-assembled polyelectrolyte complexes, the arrangements of polyaniline chains within the self-assembled conducting domains are often disordered as a result of coiling and the polydispersity of the chains. It was demonstrated with polybenzylglutamates and related polymers that polydispersity can affect the overall structure: polydispersity leads to nematic order, whereas monodispersity leads to smectic order.[7]

Oligoanilines with well-defined chain lengths are model compounds for the electronic, magnetic, optical, and structural properties of PANI.[8] For instance, the conductivity values for the complexes of tetrameric and octameric anilines with HCl are approximately 3×10^{-3} and $1\,S\,cm^{-1}$, respectively.[9,10] More importantly, as their assembly can be precisely controlled owing to their monodispersity and better solubility, they may also exhibit novel properties.[11]

Phenyl-capped tetraaniline (TANI) and phenyl-capped octaaniline (OANI) were prepared by using slight modifications of reported methods[10,12] (see Supporting Information for details). Polyaniline ($M_w = 28000$) was provided by PANIPOL Ltd. and was synthesized by a conventional method.[13] The surfactant di(undecenyl) phosphate (ωC11) was prepared according to a general procedure employed for the synthesis of di(*n*-alkyl) phosphates.[14] Bis(2-ethylhexyl) phosphate (BEHP) was obtained from Aldrich. The complexes of oligoaniline and PANI with the phosphate surfactants were prepared by dissolving TANI, OANI, or PANI and the surfactants in a common solvent (usually formic acid, but chloroform for the complexes of TANI) followed by film casting. Different molar ratios (x) of surfactant to aniline groups were used, and the complexes are denoted as [TANI(BEHP)$_x$] as an example. The nominally fully doped case corresponds to $x = 0.5$ in which all the imine nitrogen atoms have been protonated by the acid. The structures of the oligoanilines and their complexes are shown in Figure 1.

In the case of TANI complexes, the most distinct effect is that upon addition of BEHP or ωC11 surfactants, the originally crystalline TANI oligomers became softened but were still birefringent, which indicates liquid crystallinity. WAXS (wide-angle X-ray scattering) investigations of [TANI(BEHP)$_x$], $x = 0.25$, 0.42, and 0.5, reveal a narrow scattering peak near $2\theta = 4.1°$ and up to five equally spaced higher order reflections which indicate highly ordered lamellar structures with a spacing of $d_1 = 2.22$ nm (see Supporting Information for 1D WAXS and SAXS (small-angle X-ray scattering) diffractograms). Increasing the molar ratio of surfactant to aniline groups, x, caused only a slight increase in the spacing. Furthermore, two much broader peaks are present at 25° ($d = 0.35$ nm) and 20° ($d = 0.45$ nm). These are attributed to the van der Waals distances between the aromatic rings of TANI (stack height calculated to be at least 16 nm in the case of [TANI(BEHP)$_{0.5}$]) and between the aliphatic chains of the dopants, respectively.[6]

1D SAXS analyses at room temperature indicated a richer supramolecular structure beyond the plain lamellar order, as demonstrated in Figure 2 for [TANI(BEHP)$_{0.5}$]. To assign the reflections, efforts were made to align the structures by

[*] Dr. Z. Wei, Dr. B. Smarsly, Dr. C. F. J. Faul[+]
Max Planck Institute of Colloids and Interfaces
Research Campus Golm
14424 Potsdam (Germany)
E-mail: charl.faul@bristol.ac.uk
T. Laitinen, Prof. O. Ikkala
Helsinki University of Technology
Department of Engineering Physics and Mathematics and
Center for New Materials
P.O. Box 2200, 02015 HUT, Espoo (Finland)
[+] New address: School of Chemistry
Inorganic and Materials Chemistry Section
University of Bristol
Bristol BS8 1TS (UK)
Fax: (+44) 117-929-0509

[**] This work was supported as part of the European Science Foundation Collaborative Research (EUROCORES) Programme on Self-Organised NanoStructures (SONS). The MPG and the Academy of Finland are acknowledged. PANIPOL Ltd is acknowledged for providing polyaniline, and VTT Microelectronics is acknowledged for the permission to use their impedance analyzers. Tapio Mäkelä, Mari Tiitu, Teemu Ruotsalainen, and Dr. Evgeny Polushkin are acknowledged for discussions and experimental assistance. The work was partly carried out in the Centre of Excellence of Finnish Academy (Bio- and Nanopolymers Research Group, 77317).

Supporting information for this article is available on the WWW under http://www.angewandte.org or from the author.

 DOI: 10.1002/ange.200460928

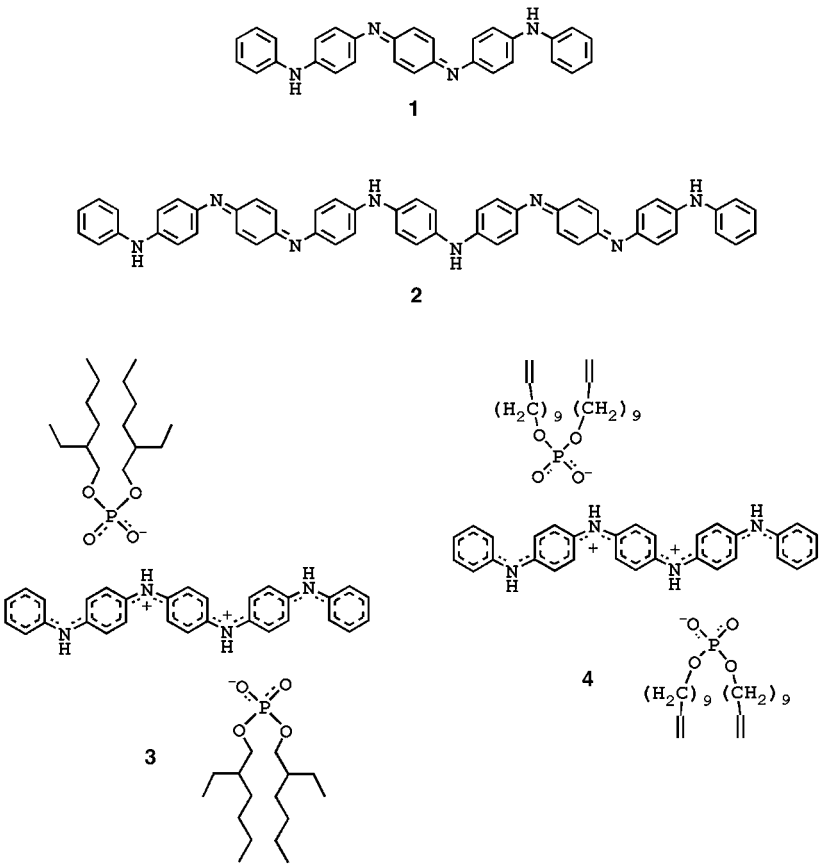

Figure 1. TANI (**1**), OANI (**2**), [TANI(BEHP)$_{0.5}$] (**3**), and [TANI(ωC11)$_{0.5}$] (**4**).

shearing the samples manually. This produced materials that were oriented to some degree. Figure 2A shows a typical 2D SAXS pattern of a manually oriented sample of [TANI(BEHP)$_{0.5}$] in which the reflections are no longer radially averaged (isotropic Debye–Scherrer patterns) but are concentrated in certain directions. Even if complete orientation with spotlike reflections was not achieved, the data quality is still sufficient to extract the angle φ from the arclike reflections (see Figure 2B for the definition of φ). For better visualization, the observed SAXS reflections are illustrated in Figure 2B (only one quadrant is shown). On the basis of a careful analysis of the anisotropic SAXS patterns, nine reflections could be determined with sufficient accuracy; that is, the position of the reflections (see the 1D pattern, Figure 2C) and the corresponding angle φ. The angles φ could only be determined with an accuracy of about 10–15°, which limits the accuracy of the structure model. Reflection i is quite broad and probably results from a superposition of two interferences. Reflection g does not show a significant degree of preferred orientation, which, however, could be a result of the limited resolution of our detector device for low scattering intensities. Hence, the main reflections can be classified into three groups with respect to the angle φ (see Table 1).

Interestingly, several families of reflections can be identified in the 2D SAXS patterns. Within a

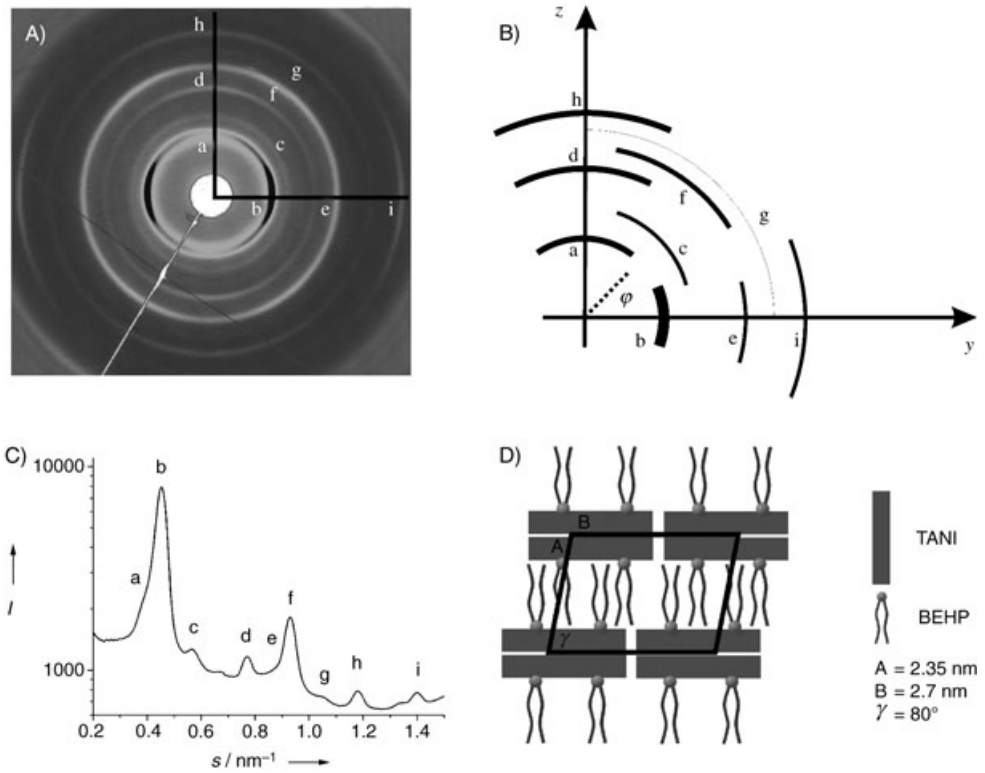

Figure 2. A) 2D SAXS pattern of an oriented sample of [TANI(BEHP)$_{0.5}$]. B) Diagram of the anisotropic scattering patterns. C) Radially averaged 1D pattern of part (A). D) Representation of the 2D columnar phase and possible packing of [TANI(BEHP)$_{0.5}$] units within the unit cell.

Table 1: Assignment of the observed SAXS reflections.

Reflections	s [nm^{-1}]	φ_{exp} [°]	$\varphi_{theoretical}$ [°]	Indexation
a	0.375	80–90	81	(01)
b	0.454	0–10	0	(10)
c	0.57	40–50	49	(11)
d	0.76	80–90	81	(02)
e	0.89	0–10	0	(20) (+(1–2))
f	0.92–0.95	55–65	66	(12) (+(2–1))
g	1.03–1.05	n.a.	49	(21)
h	1.18	80–90	81	(03)
i	1.34	0–10	0	(30) (+(13))

certain variance, $\varphi = 80$–$90°$ for reflections a, d, and h, whereas for b and e $\varphi = 0°$. Also for i we found $\varphi = 0°$, but this reflection is superimposed with another reflection. Hence, a reasonable interpretation is that b and e belong to a (hk0) family and a, d, and h belong to the (001) family. In general, unambiguous assignments are difficult owing to the limited number of reflections and the experimental uncertainty in φ. However, as only one type of reflection is observed on the y axis (multiples of the first interference), this indicates that the present system can be regarded as a 2D mesostructure. Therefore it seems legitimate to assume that the reflections on the y axis correspond to the (h0) lattice planes of a 2D structure that lacks mesoscale periodicity in the third dimension. Within this model, the reflections in the z direction reduce to the (01) family. Furthermore, as a common feature of mesostructures in general, the symmetry of these morphologies is quite low so that usually the first-order reflections are indeed observable.

On the basis of these assumptions, the positions of all reflections can be reasonably well indexed to a 2D unit cell in the form of a parallelogram with parameters $\gamma = 80°$, $A = 2.35$ nm, and $B = 2.7$ nm (see Table 1 for the indexation). Several reflections cannot be assigned as distinguishable interferences (e.g. (1–2)) because the corresponding positions probably coincide with other reflections. This effect could explain the observation that several arcs in the 2D pattern apparently smear into a ring, which would simply be a consequence of the superposition of different reflections. In particular, this structure model accounts well for the angles φ of the off-axis reflections, c and f, which is crucial for a reasonable structure model.

Whereas, theoretically, for nonrectangular lattices, the (01) reflections cannot be located on the z axes, in the present case, the slight deviation from a rectangular lattice ($\approx 10°$) is difficult to detect in the 2D SAXS patterns.

In essence, this unit cell can be regarded as a slightly distorted 2D rectangular lattice and is similar to the columnar phases recently reported by Tschierske and co-workers for calamitic bolaamphiphiles.[15] The A parameter of the unit cell also fits very well with an interdigitated arrangement of the surfactant tails, whereas the B parameter fits with the calculated length of the salt form of a TANI molecule (see Figure 2D and Supporting Information). Furthermore, from the volume (2.22 nm^3) of a unit cell of 0.35-nm thickness (corresponding to the π–π stacking distance), the number of molecules was calculated and corresponds to the presence of two complexed TANI units (the volume of a [TANI-$(BEHP)_{0.5}$] unit is 1.10 nm^3 from calculations performed with CeriusII software).

Even if this interpretation allows the reflections to be indexed in a reasonable manner, owing to the limited number of reflections this structure analysis cannot be regarded as unambiguous. From the evaluation of 1D SAXS data, the second phosphate surfactant ωC11 forms quantitatively similar structures upon complexation with tetraaniline.

The driving force for the 2D columnar structures in [TANI$(BEHP)_x$] and [TANI$(\omega C11)_x$] was next addressed. TANI is a rigid molecule as a result of its conjugated structure. Upon complexation with the phosphoric acid surfactant, it can be regarded as a supramolecule in which the soft alkyl side chains are attached to the hard TANI backbone by ionic bonds. Liquid crystallinity is therefore expected as already seen in the case of perylenediimide-based materials[16] or other rigid-core materials that contain several incompatible molecular parts.[15] Although the columnar structure is reminiscent of smectic phases found for calamitic structures, the arrangement of the molecules is slightly different as very efficient stacking of the TANI molecules in [TANI$(BEHP)_x$] and [TANI$(\omega C11)_x$] is observed as a result of the strong π–π interactions (WAXS studies). These systems can therefore be seen to represent the noncovalent analogues of semifluorinated rodlike systems, with strong segregation within the molecule driving the formation of the 2D columnar phase structures. The ordering of tetraaniline within the self-assembled layers is also supported by the crystalline structure of the surfactant-free analogue, HCl-doped tetraaniline ([TANI$(HCl)_{0.5}$]). A spacing $d = 2.58$ nm, nearly the same as that of [TANI$(BEHP)_{0.5}$], was also observed, as determined by the length of the TANI molecule.

The previous discussion showed that the 2D columnar phase structure in the oligoaniline–phosphate surfactant complexes is ascribed to the monodispersity of both of the building blocks; that is, the main chains and the surfactants. As PANI is polydisperse, stacking of its surfactant complexes is therefore not expected. Interestingly, [PANI$(BEHP)_{0.5}$] self-assembles to form a highly ordered hexagonal structure, unlike the rectangular columnar phase of the corresponding oligomeric [TANI$(BEHP)_{0.5}$]. The different self-assembly of PANI and TANI may be ascribed to their different conformations. PANI displays a coil-like conformation, which therefore takes more "lateral" space and thus forms hexagonal structures in the direction of the chains. The possibility of π–π stacking (and therefore an added driving force to form side-by-side arrangements) is therefore reduced considerably. TANI, on the other hand, is rodlike and short and thus takes much less lateral space with consequent higher possibilities for π–π stacking. Such conclusions are supported by the complexes of the rigid rodlike conjugated polymer poly(2,5-pyridinediyl) (PPY) and PANI with camphor sulfonic acid (CSA) and hexylresorcinol (Hres): [PPY$(CSA)_{0.5}(Hres)_{1.0}$] forms a lamellar self-assembly, whereas the corresponding PANI complexes form a cylindrical self-assembly.[6b,17]

Surprisingly, a mixture of both lamellar and hexagonal structures are observed in [OANI$(BEHP)_{0.5}$], as shown in

Figure 3A, even if no clear macroscopic phase separation was observed by means of an optical microscope (after annealing at high temperatures). The *d* spacing of the hexagonal structure is 2.89 nm, which is very similar to the value found

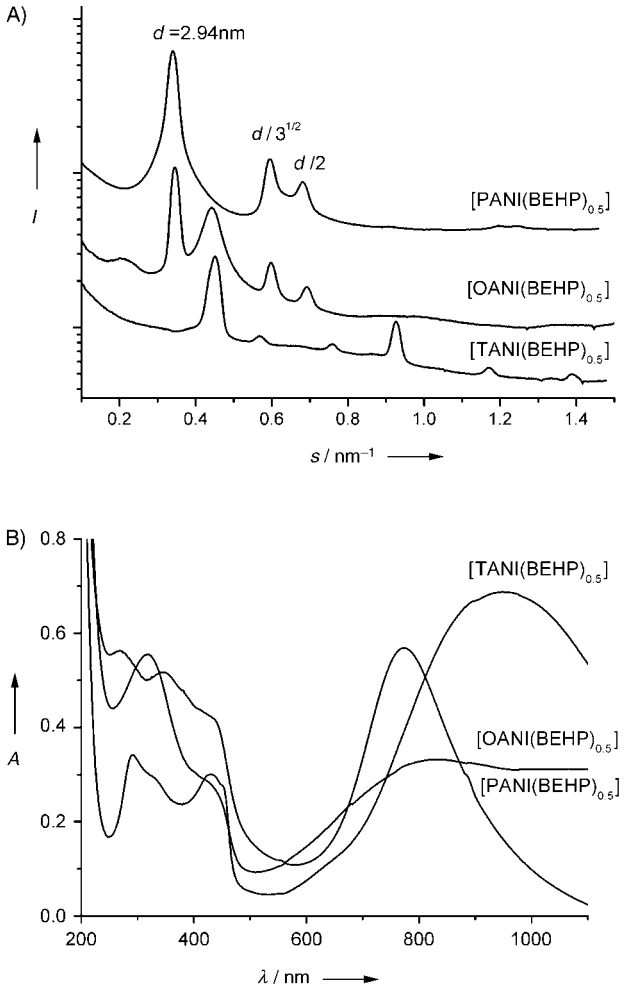

Figure 3. The effect of aniline chain length in [PANI(BEHP)$_{0.5}$], [OANI(BEHP)$_{0.5}$], and [TANI(BEHP)$_{0.5}$]. A) SAXS. B) UV/Vis spectra.

for [PANI(BEHP)$_{0.5}$] (2.94 nm), whereas the other structure has a *d* spacing of 2.25 nm, which is nearly the same as the value found in [TANI(BEHP)$_{0.5}$] (2.22 nm). This observation may indicate that OANI is a limiting case in which the coexistence of the behavior of a rodlike molecule (similar to TANI) and a coil-like conformation (similar to PANI) is found. Furthermore, another strong peak that corresponds to a *d* spacing of 4.88 nm is observed. This is slightly longer than the length calculated for the phenyl-capped octaaniline molecules (4.48 nm in the doped state, see Supporting Information). If the effect of the molecular stacks separated by surfactants is considered, the length corresponds to the expected length of the complexes.

The UV/Vis spectra of BEHP-doped complexes for aniline chains of different lengths are shown in Figure 3B. All spectra show three absorption maxima at approximately $\lambda = 300$, 400, and > 700 nm, which are ascribed to the π–π^* transition of the benzenoid ring (300 nm) and the absorption band of polarons.[18] However, their positions and relative strengths are totally different. The polaron absorption maximum of TANI is located at approximately $\lambda = 950$ nm and extends to higher wavelengths, whereas that of PANI is located at about $\lambda = 775$ nm and tails off beyond that value. This suggests that the tetraaniline chains are in an extended rodlike conformation, whereas polyaniline chains are coiled. The corresponding maximum of the OANI complex is located at $\lambda = 830$ nm and extends to higher wavelength, and the behavior is, once again, between that of TANI and PANI. Therefore, in conclusion, TANI is in a rodlike conformation, PANI is in a coiled conformation, and OANI is a limiting case with a combination of the two behaviors.

Both [TANI(ωC11)$_x$] and [TANI(BEHP)$_x$] lose birefringence upon heating beyond 70–80 °C and 80–95 °C, respectively (see the Supporting Information for representative differential scanning calorimetry (DSC) curves). This indicates that the complexes are disordered at high temperatures. This is also supported by SAXS which revealed no pronounced scattering peaks at elevated temperature. These transitions show a very interesting connection to the electrical conductivity. We made an initial effort to analyze the electrical conductivities of the oligomer–surfactant complexes by using the standard four-wire method. However, the complexes did not display linear voltage–current relationships and therefore were not purely Ohmically conducting; that is, they were not purely electronic conductors. Thus, ac-impedance spectroscopy was employed by using an impedance analyzer (HP 4192LF) at frequencies from 0.01 to 1000 kHz. The dc conductivities were determined by using standard procedures.[19]

The complexes [TANI(ωC11)$_x$] showed pronounced conductivity transitions as a function of temperature (see Figure 4A). At room temperature, the conductivity of [TANI(ωC11)$_{0.42}$] is of the order of 3×10^{-3} S cm^{-1}. An increase in the temperature to beyond 70 °C leads to an abrupt drop in the conductivity by three orders of magnitude. The transition is reversible in consecutive cooling and heating cycles with some hysteresis observed. A slightly larger transition was observed for $x = 0.5$. For smaller values of x, such as $x = 0.25$ or 0.33, the drop in conductivity is significantly smaller. For $x = 1.0$, no transition was observed. Smaller thermal conductivity switching was also observed in [TANI(BEHP)$_x$] complexes, but not for the OANI or PANI complexes.

To explain the conductivity transition, the question was posed whether tetraaniline was dedoped upon heating. The UV/Vis spectra at different temperatures were thus measured and showed that there was little decrease in the polaron absorption (Figure 4B) which indicates no dedoping. However, the conductivity of [TANI(ωC11)$_x$] can be correlated with the extent of order found within the self-assembled material. Figure 4B shows that the integrated intensity of the first diffraction peak of the columnar structures decreased upon increasing the temperature past 70 °C, which corresponds to the order–disorder transition temperature. Similar temperature-dependent behavior is observed for the conduc-

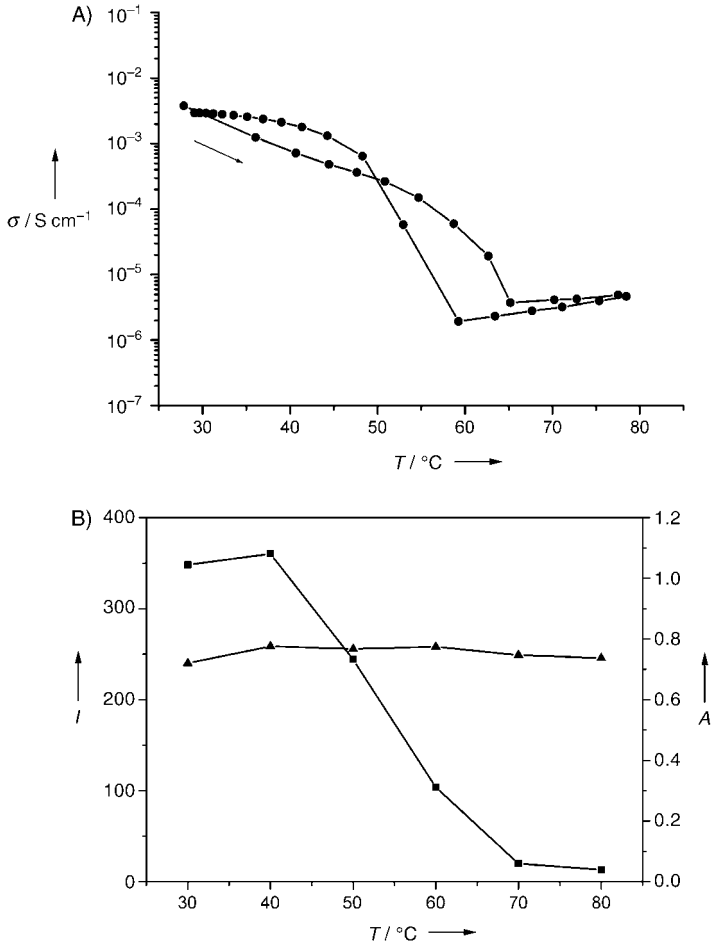

Figure 4. Correlation between conductivity and self-assembly for [TANI(ωC11)$_{0.42}$]. A) The dc conductivity as a function of temperature (temperature sweep: 1 °C min^{-1}). B) Integrated X-ray scattering peak height of the first-order reflection ($s = 0.42$ nm^{-1}) and the UV/Vis absorption at the polaron peak maximum as a function of temperature ■ = SAXS, ▲ = UV/Vis.

tivity as seen in Figure 4 A. This indicates that the conductivity switching for [TANI(ωC11)$_x$] can be assigned to the order–disorder transition from an ordered 2D columnar structure to a disordered state. In this transition, the degree of organization between the conducting layers decreases and the disorder limits the carrier mobility of the interchain electron transfer, which thus leads to a dramatic decrease in the electrical conductivity.[20] A similar but much smaller effect is observed for [TANI(BEHP)$_x$] and we are at present trying to explain the difference between the two complexes.

In summary, a 2D rectangular columnar structure based on oligoanilines was prepared by using double-tail phosphate surfactants. In this structure, the conducting layers of oligoanilines are segregated by the insulating layers of the dialkyl phosphates. The oligoaniline molecules, owing to their monodispersity, form well-ordered infinite 2D columnar stacks within the conducting layers. Upon heating, the tetraaniline complexes showed an order–disorder transition from this 2D phase structure to a disordered state: This transition corresponds to a large reversible change in the electrical conductivity. This research shows that functional and externally controllable electroactive nanostructures can be obtained by an ionic self-assembly process.

Received: June 10, 2004
Revised: September 29, 2004
Published online: December 21, 2004

Keywords: conducting materials · liquid crystals · nanostructures · self-assembly · surfactants

[1] a) S. W. Lee, C. Mao, C. E. Flynn, A. M. Belcher, *Science* **2002**, *296*, 892; b) A. Bachtold, P. Hadeky, T. Nakanish, C. Dekker, *Science* **2001**, *294*, 1317; c) S. Fan, M. G. C. Hapline, N. R. Franklin, T. W. Tombler, A. M. Cassell, H. Dai, *Science* **1999**, *283*, 512.

[2] a) G. M. Whitesides, J. P. Mathias, C. T. Seto, *Science* **1991**, *254*, 1312; b) G. M. Whitesides, B. Grzybowski, *Science* **2002**, *295*, 2418.

[3] a) O. Ikkala, G. ten Brinke, *Science* **2002**, *295*, 2407; b) C. F. J. Faul, M. Antonietti, *Adv. Mater.* **2003**, *15*, 673; c) V. Percec, M. Glodde, T. K. Bera, Y. Miura, I. Shiyanovskaya, K. D. Singer, V. S. K. Balagurusamy, P. A. Heiney, I. Schnell, A. Rapp, H.-W. Spiess, S. D. Hudson, H. Duan, *Nature* **2002**, *419*, 384; d) G. M. Whitesides, B. Grzybowski, *Science* **2002**, *295*, 2418; e) T. Kato, *Science* **2002**, *295*, 2414.

[4] J. Ruokolainen, R. Mäkinen, M. Torkkeli, T. Mäkelä, R. Serimaa, G. ten Brinke, O. Ikkala, *Science* **1998**, *280*, 557.

[5] a) *Electronic Materials: The Oligomer Approach*, (Eds.: G. Wegner, K. Müllen), Wiley-VCH, Weinheim, **1996**; b) C. Joachim, *Nanotechnology* **2002**, *13*, R1.

[6] a) W.-Y. Zheng, R.-H. Wang, K. Levon, Z. Y. Rong, T. Taka, W. Pan, *Macromol. Chem. Phys.* **1995**, *196*, 2443; b) A. Pron, P. Rannou, *Prog. Polym. Sci.* **2002**, *27*, 135; c) H. Kosonen, J. Ruokolainen, M. Knaapila, M. Torkkeli, K. Jokela, R. Serimaa, G. ten Brinke, W. Bras, A. P. Monkman, O. Ikkala, *Macromolecules* **2000**, *33*, 8671; d) B. Dufour, P. Rannou, D. Djurado, H. Janeczek, M. Zagorska, A. de Geyer, J.-P. Travers, A. Pron, *Chem. Mater.* **2003**, *15*, 1587.

[7] a) S. M. Yu, V. P. Conticello, G. Zhang, C. Kayser, M. J. Fournier, T. L. Mason, D. A. Tirrell, *Nature* **1997**, *389*, 167; b) H. Schlaad, B. Smarsly, M. Losik, *Macromolecules* **2004**, *37*, 2210.

[8] a) J. Libert, J. Cornil, D. A. dos Santos, J. L. Bredas, *Phys. Rev. B* **1997**, *56*, 8638; b) A. G. MacDiarmid, Y. Zhao, J. Feng, *Synth. Met.* **1999**, *100*, 131.

[9] W. Zhang, J. Feng, A. G. MacDiarmid, A. J. Epstein, *Synth. Met.* **1997**, *84*, 119.

[10] F.-L. Lu, F. Wudl, M. Nowak, A. J. Heeger, *J. Am. Chem. Soc.* **1986**, *108*, 8311.

[11] a) S. Quillard, B. Corraze, M. Poncet, J.-Y. Mevellec, J.-P. Buisson, M. Evain, W. Wang, A. G. MacDiarmid, *Synth. Met.* **2003**, *137*, 921; b) X. Chen, S. Liu, Y. Song, S. Dong, *Chem. Lett.* **2002**, 552.

[12] J. Gao, K. Li, W. Zhang, C. Wang, Z. Wu, Y. Ji, Y. Zhou, M. Shibata, R. Yosomiya, *Macromol. Rapid Commun.* **1999**, *20*, 560.

[13] Y. Cao, A. Andreatta, A. J. Heeger, P. Smith, *Polymer* **1989**, *30*, 2305.

[14] a) T. Kunitake, Y. Okahata, *Bull. Chem. Soc. Jpn.* **1978**, *51*, 1877; b) D. Ganeva, C. F. J. Faul, C. Götz, R. D. Sanderson, *Macromolecules* **2003**, *36*, 2862.

[15] a) M. Prehm, S. Diele, M. K. Das, C. Tschierske, *J. Am. Chem. Soc.* **2003**, *125*, 614; b) X. H. Cheng, M. K. Das, S. Diele, C. Tschierske, *Angew. Chem.* **2002**, *114*, 4203; *Angew. Chem. Int.*

Ed. **2002**, *41*, 4031; c) M. Prehm, X. H. Cheng, S. Diele, M. K. Das, C. Tschierske, *J. Am. Chem. Soc.* **2002**, *124*, 12072.
[16] a) Y. Guan, Y. Zakrevskyy, J. Stumpe, M. Antonietti, C. F. J. Faul, *Chem. Commun.* **2003**, 894; b) Y. Zakrevskyy, C. F. J. Faul, Y. Guan, J. Stumpe, *Adv. Funct. Mater.* **2004**, *14*, 835.
[17] M. Knaapila, M. Torkkeli, L. E. Horsburgh, L.-O. Pålsson, K. Jokela, R. Serimaa, G. ten Brinke, A. P. Monkman, O. Ikkala, *Appl. Phys. Lett.* **2002**, *81*, 1489.
[18] a) A. G. MacDiarmid, A. J. Epstein, *Synth. Met.* **1994**, *65*, 103; b) L. Dai, J. Lu, B. Matthews, A. W. H. Mau, *J. Phys. Chem. B* **1998**, *102*, 4049.
[19] A. K. Jonscher, *Dielectric Relaxation in Solids*, Chelsea Dielectric, London, **1983**.
[20] K. Lee, A. J. Heeger, *Synth. Met.* **2002**, *128*, 279.

